Published in final edited form as:
Neuropharmacology. 2011 ; 61(1-2): 12–24. doi:10.1016/j.neuropharm.2011.02.010.

Multiple Protein Kinases Determine the Phosphorylated State of the Small Heat Shock Protein, HSP27, in SH-SY5Y Neuroblastoma Cells

Linda A. Dokas[*,a], **Amy M. Malone**[a], **Frederick E. Williams**[a], **Surya M. Nauli**[a,b], and **William S. Messer Jr**[a,b]

Amy M. Malone: amalone426@hotmail.com; Frederick E. Williams: frederick.williams2@utoledo.edu; Surya M. Nauli: surya.nauli@utoledo.edu; William S. Messer: william.messer@utoledo.edu

[a]Department of Pharmacology, College of Pharmacy, 3000 Arlington Avenue, The University of Toledo, Toledo OH 43614 USA

[b]Department of Medicinal & Biological Chemistry, College of Pharmacy, 3000 Arlington Avenue, The University of Toledo, Toledo OH 43614 USA

Abstract

In SH-SY5Y human neuroblastoma cells, the cholinergic agonist, carbachol, stimulates phosphorylation of the small heat shock protein 27 (HSP27). Carbachol increases phosphorylation of both Ser-82 and Ser-78 while the phorbol ester, phorbol-12, 13-dibutyrate (PDB) affects only Ser-82. Muscarinic receptor activation by carbachol was confirmed by sensitivity of Ser-82 phosphorylation to hyoscyamine with no effect of nicotine or bradykinin. This response to carbachol is partially reduced by inhibition of protein kinase C (PKC) with GF 109203X and p38 mitogen-activated protein kinase (MAPK) with SB 203580. In contrast, phosphorylation produced by PDB is completely reversed by GF 109203X or CID 755673, an inhibitor of PKD. Inhibition of phosphatidylinositol 3-kinase or Akt with LY 294002 or Akti-1/2 stimulates HSP27 phosphorylation while rapamycin, which inhibits mTORC1, does not. The stimulatory effect of Akti-1/2 is reversed by SB 203580 and correlates with increased p38 MAPK phosphorylation. SH-SY5Y cells differentiated with a low concentration of PDB and basic fibroblast growth factor to a more neuronal phenotype retain carbachol-, PDB- and Akti-1/2-responsive HSP27 phosphorylation. Immunofluorescence microscopy confirms increased HSP27 phosphorylation in response to carbachol or PDB. At cell margins, PDB causes f-actin to reorganize forming lamellipodial structures from which phospho-HSP27 is segregated. The resultant phenotypic change in cell morphology is dependent upon PKC, but not PKD, activity. The major conclusion from this study is that the phosphorylated state of HSP27 in SH-SY5Y cells results from integrated signaling involving PKC, p38 MAPK and Akt.

1. Introduction

The small heat shock protein, HSP27 (HSPB1), promotes neuronal survival (Latchman, 2005), a function well characterized in sensory neurons (Lewis et al., 1999; Dodge et al.,

[*]Corresponding Author: Current Address: Linda A. Dokas, Ph.D., Molecular and Behavioral Neuroscience Institute, 205 Zina Pitcher Place, University of Michigan, Ann Arbor MI 48109, Telephone: 734-936-3651, FAX: 734-647-4130, ldokas@umich.edu.

2006). In brain, HSP27 is induced by heat shock and other insults (Akbar et al., 2001; Bechtold and Brown, 2003) and is neuroprotective in experimental models of epilepsy, stroke and amyotrophic lateral sclerosis *in vivo* (Akbar et al., 2003; Badin et al., 2006; Sharp et al., 2008). Both constitutive and induced levels of HSP27 may limit neuronal vulnerability to neurodegenerative states (Klettner, 2004; Chen and Brown, 2007). For example, HSP27 associates with plaques and tangles in the Alzheimer's disease brain and protects against β-amyloid- or phosphorylated tau-induced cell pathology (Shimura et al., 2004; King et al., 2009; Koren et al., 2009).

Signal transduction pathways regulate the phosphorylated state of HSP27 at three major sites (Ser-15, Ser-78 and Ser-82 in the human sequence) through the activities of sequential protein kinases, principally p38 mitogen-activated protein kinase (MAPK)/MAPK-activated protein kinase-2 (MAPKAPK-2; also termed MK2) and protein kinase C (PKC)/protein kinase D (PKD) (Kostenko and Moens, 2009). Although anti-apoptotic and adaptive functions of HSP27 depend upon its phosphorylated state (Lavoie et al., 1993 and 1995; Rogalla et al., 1999; Benn et al., 2002; Geum et al., 2002), relatively little is known regarding factors that modulate HSP27 phosphorylation once it is expressed in neurons.

The SH-SY5Y cell line is an N-type neuroblastoma that can be differentiated to a more physiological phenotype while expressing endogenous HSP27 and muscarinic receptors, predominantly the M_3 subtype (Lambert et al., 1989; Lavenius et al., 1994). M_3 receptors on various cell lines activate PKC, extracellular signal-regulated protein kinase 1/2 (ERK1/2), phosphatidylinositol 3-kinase (PI3-K) and Akt (Slack, 2000; Tang et al., 2002; Anger et al., 2007; Rosethorne et al., 2008). Signal transduction pathways involving these protein kinases regulate gene expression and cytoskeletal dynamics in SH-SY5Y cells while activation of $G_{q/11}$ receptors on these cells broadly protects against apoptosis induced by diverse injurious stimuli (Rösner et al., 1995; DeSarno et al., 2003; Mookherjee et al., 2007; Rössler et al., 2008). Such end points are also modulated by HSP27 (Landry and Huot, 1999; Benn and Wolf, 2004). A precedent for muscarinic receptor-coupled HSP27 phosphorylation exists in smooth muscle where it induces association of contractile proteins and PKC with elements of the cytoskeleton (Reviewed in Gerthoffer, 2005).

As part of its anti-apoptotic and chaperone functions, HSP27 stabilizes the actin-based cytoskeleton during periods of stress (Lavoie et al, 1995; Geum et al., 2002; Landry and Huot, 1999) and modulates actin filament dynamics related to cell structure and motility (Lavoie et al., 1993; During et al., 2007). In SH-SY5Y cells, cholinergic receptor stimulation or a phorbol ester cause rapid reorganization of the actin-based cytoskeleton in a PKC-dependent manner that may mediate cell motility and/or secretion of catecholamine from dense-cored vesicles (Rösner et al., 1995; Viviani et al., 1996; Danks et al., 1999). Therefore, in the SH-SY5Y neuroblastoma model system, the signal transduction pathways initiated by muscarinic receptor activation or the phorbol ester, phorbol-12, 13-dibutyrate (PDB) have been compared with three principal goals: 1.) To characterize phosphorylation of endogenous HSP27 as it is coupled to muscarinic receptor activation before and after differentiation with a phorbol ester and growth factor; 2.) To identify the protein kinases involved in phosphorylation of HSP27, principally at Ser-82, a site critical for the protein:protein interactions that mediate its functions (Lambert et al., 1999); and 3.) To determine whether HSP27 phosphorylation correlates with a functional response, i.e., reorganization of the actin-based cytoskeleton.

2. Materials and methods

2.1 Materials

Dulbecco's Modification of Eagle's Medium (DMEM), 1X with 4.5 g/L of glucose, 584 mg/L of l-glutamine and 110 mg/L of sodium pyruvate, was obtained from Mediatech Inc., Herndon, VA, USA. Premium 0.1 μm-filtered fetal bovine serum (FBS) was a product of Atlanta Biologicals, Atlanta, GA, USA. Penicillin (10,000U/mL)/streptomycin (10,000 μg/mL), trypsin/EDTA (1X, 0.05%), recombinant human basic fibroblast growth factor (bFGF) and rhodamine phalloidin were purchased from Invitrogen, Carlsbad, CA, USA. Hyoscyamine and Triton X-100 were obtained from Sigma-Aldrich Corp., St, Louis, MO, USA. All protein kinase modulators, nicotine ditartrate and bradykinin were products of EMD Biosciences (Calbiochem), LaJolla, CA, USA, with the exception of CID 755673 that was from Tocris Bioscience, Ellisville MO, USA. Anti-rabbit and anti-mouse alkaline phosphatase-conjugated secondary antibodies and Passive Lysis Buffer (PLB; supplied as a 5X concentrated stock and diluted just before use) were from Promega Corporation, Madison, WI, USA. Bovine serum albumin (BSA), carbamoylcholine chloride (carbachol, CCh), dimethyl sulfoxide (DMSO), sorbitol and the anti-phospho-(Ser-85) and -(Ser-15) primary antibodies used for immunoblotting and immunofluorescence microscopy were purchased from Fisher Scientific, Waltham MA. (Note that Ser-85 in the sequence of rat HSP27 corresponds to Ser-82 in the human sequence.). The anti-phospho-(Ser78) primary antibody was a product of Epitomics, Inc., Burlingame, CA. Phospho-specific primary antibodies to ERK1/2 (Thr-202/Tyr-204), p38 MAPK (Thr-180/Tyr-182), Akt (Ser-473) and S6 ribosomal protein (Ser235/236) were products of Cell Signaling Technology, Inc., Danvers, MA, USA, as were pan-antibodies to total ERK1/2, p38 MAPK and Akt. Total HSP27 was detected with a primary antibody from Enzo Life Sciences, Plymouth Meeting, PA, USA. Polyvinylidene fluoride (PVDF) membrane and preimmune rabbit IgG were products of Millipore Corp., Inc, Billerica, MA, USA. Fluorescein-conjugated anti-rabbit IgG (H + L) and Vectashield Hard Set™ Mounting Medium with DAPI (4',6-diamidino-2-phenylindole) were purchased from Vector Laboratories, Burlingame CA, USA. Paraformaldehyde was obtained from Electron Microscopy Services, Hatfield PA, USA, as a 16% aqueous solution.

2.2 Culture and treatment of cells

The SH-SY5Y cell line (ATCC #CRL-2266™) is a N-type human neuroblastoma derived from a metastatic bone tumor that expresses muscarinic cholinergic receptors, principally the M_3 subtype (Ross et al., 1983; Lambert et al., 1989). Cells were maintained in DMEM-10% FBS-50U/mL of penicillin/50 μg/mL of streptomycin and subpassaged at weekly intervals with change of the medium every 3–4 days. Prior to an experiment, cells were plated at a density of 8×10^5 cells per uncoated 60 mm polystyrene plate. After 2 days in culture, the medium was replaced with serum-free DMEM without penicillin/streptomycin for 60 min prior to the start of an experiment. Hyoscyamine (the active enantiomer of atropine) or protein kinase inhibitors, as specified in Table I, were added at the beginning of this preincubation. The time of incubation with CCh and its concentration were as indicated in specific experiments. Hyoscyamine and CCh were dissolved in DMEM and an equal volume of medium was added to control plates. Protein kinase modulators and PDB were solubilized in DMSO. The effects of PDB were analyzed under two conditions: after addition for the last 15 min of the preincubation at a concentration of 1 μM or for 2 hr after the end of the preincubation at a concentration of 10 nM. A comparable volume of DMSO was added to control incubations. In all cases, the concentration of DMSO in the incubations was less than 0.5%. Basal phosphorylation was defined as that measured in control incubations containing equal volumes of the DMEM and/or DMSO vehicles. For imaging with phase contrast microscopy, cells were cultured at a lower density (4×10^5 per

60 mm polystyrene plate) for two days. The medium was replaced with serum-free DMEM for 60 min with or without protein kinase inhibitors prior to addition of PDB or DMSO vehicle as described above.

The effect of hyperosmotic stress on HSP27 phosphorylation was determined by preincubating cells in serum-free DMEM for 30 min. At this time, medium was replaced with fresh serum-free DMEM (control) or serum-free DMEM containing 0.3M sorbitol to produce hyperosmotic conditions and the incubation was continued for an additional 30 min before preparation of cell lysates. When added in such experiments, SB 203580 was maintained at a concentration of 10 μM through both phases of the 60 min incubation.

The protocol of Lavenius et al. (1994) was used to differentiate SH-SY5Y cells to a mature neuronal phenotype. Cells were plated at a density of 1 § 10^5 cells per well of a 6-well plate in 2 ml of DMEM-10% FBS-penicillin/streptomycin. After 24 hr, the medium was changed to serum-free DMEM and PDB and bFGF were added to final concentrations of 16 nM and 3 nM, respectively. Cells were grown under these conditions for 5 days with one change of medium and PDB/bFGF. Experiments were initiated by replacement of serum-free DMEM and addition of hyoscyamine, protein kinase inhibitors, CCh and PDB as specified in the text.

2.3 Protein analysis

Cell lysates were prepared using 1X PLB according to the manufacturer's specifications and stored at −20 °C prior to immunoblotting. Samples containing equal amounts of protein were resolved with SDS-polyacrylamide gel electrophoresis (SDS-PAGE). Proteins were transferred to PVDF membrane. A 20 min transfer was used in the case of HSP27, a 30 min transfer for ERK1/2 or p38 MAPK and a 45 min transfer for Akt, based on the relative sizes of the proteins. Following blocking of nonspecific binding sites with a solution of 2.5% dry milk-0.1% Tween-20, immunoblotting for phosphorylated proteins was performed with primary antibodies that recognize the following phosphorylation sites: HSP27, Ser-15, Ser-78 or Ser-82; ERK1/2, Thr-202/Tyr-204, p38 MAPK, Thr-180/Tyr-182, Akt, Ser-473 and S6 ribosomal protein, Ser-235/236 or with pan antibodies that recognize all isoforms of each protein. In this paper, any reference to phospho-HSP27 implies phosphorylation of Ser-82 unless otherwise stated. Immunoreactive bands were visualized using anti-rabbit or anti-mouse alkaline phosphatase-conjugated secondary antibodies. Equal loading of protein across all sample lanes of each gel was confirmed by staining the high molecular weight proteins remaining on gels after transfer to immunoblots.

2.4 Cell Imaging

To examine morphology, cells were imaged digitally using phase contrast microscopy at 20X magnification with a polarizing filter on a Zeiss Axovert 25CFL fluorescence microscope. To quantify effects of PDB ± protein kinase inhibitors on cell morphology, 50 cells per field were counted for the presence of lamellipodial profiles. A total of four fields from duplicate experiments were analyzed under each condition and results were expressed as the % of cells displaying lamellipodia.

For immunofluorescence microscopy, 5×10^4 cells were cultured on a glass cover slip per sample for two days. Following replacement of medium with serum-free DMEM for 60 min, CCh was added at a concentration of 1 mM for 5 min. Incubations with PDB were performed with a concentration of 1 μM for 15 min. Control samples contained equivalent volumes of DMEM or DMSO. At the end of the experimental treatments, cells were rinsed one time with PBS and fixed for 30 min with freshly prepared 4% paraformaldehyde in PBS. Following two washes with PBS for 5 min, cells were permeabilized in PBS-5%

BSA-0.2% Triton X-100. Cells were washed three times in PBS prior to addition of rhodamine phalloidin to a final concentration of 100 nM in PBS-2% BSA-0.2% Triton X-100 for 30 min to label filamentous (f)-actin. Cells were washed again three times with PBS. Excess PBS was blotted off the edge of the coverslips and they were sealed to microscope slides with Vectashield/DAPI.

For immunolabeling, a phospho-specific primary antibody directed against Ser-82 or an equivalent amount of rabbit preimmune IgG were added at a 1:500 dilution in PBS-5%BSA-0.2% Triton X-100 following the post-permeabilization washes. Samples were kept at 4 °C overnight. The next day, cells were washed three times with PBS. An anti-rabbit IgG secondary antibody conjugated to fluorescein was added for 60 min. Cells were washed three final times with PBS and adhered to microscope slides with Vectashield/DAPI. For double-labeling, the antibody incubations were performed after labeling of cells with rhodamine phalloidin. Images were captured with Metamorph version 7.0 software on a Nikon Ti-U microscope coupled with Photometrics Coolsnap ES2, 12 bit, 20 MHz Digital Monochrome Camera with IEEE-1394 interface. All images within one set were taken with the same exposure time and binning values.

2.5 Quantification and statistical analysis

Quantification of immunoreactivity on blots was obtained with densitometric analysis of protein bands using UN-SCAN-IT gel™ digitizing software (Version 6.1, Silk Scientific Corporation Inc., Orem UT, USA). In all cases, effects on phosphorylation were normalized to the total amount of each protein determined by immunoblotting with an antibody that recognizes both phospho- and dephospho-forms. Data are expressed as the mean ± SEM of results combined from each set of experiments. Statistical analysis was performed using Student's T-test with significance defined as $p \leq 0.05$.

3. Results

3.1 Activation of muscarinic receptors on SH-SY5Y cells increases HSP27 phosphorylation

Incubation of SH-SY5Y neuroblastoma cells with 1 mM CCh caused an increase in the phosphorylation of endogenous HSP27 as detected by immunoblotting with a phospho-specific antibody to Ser-82 (A representative immunoblot is shown in Fig. 1A). Phosphorylation of this site was analyzed since it regulates the oligomeric state of HSP27, a critical determinant of its functions (Lambert et al., 1999). Since there was no significant change in the total amount of HSP27 in the same cell lysates using a primary antibody that recognizes both phospho- and dephospho-forms of the protein, changes in phosphorylation of HSP27 were quantified as the ratio of phospho-HSP27 to total HSP27 following densitometry of immunoreactive bands. At 1–5 min of incubation with 1 mM CCh, a maximal increase in HSP27 phosphorylation was observed. Thereafter, phosphorylation of HSP27 declined but remained significantly elevated above basal levels for as long as 60 min of incubation with CCh (Fig. 1B). The effect of CCh was concentration-dependent with an EC_{50} value of approximately 10 μM (pEC_{50}, 4.97 ± 0.02) and a maximal response was obtained between 0.1 and 1 mM (Fig. 1C). For all further experiments in this study, 1 mM CCh was used in a 5 min incubation with SH-SY5Y cells.

Involvement of muscarinic receptors in stimulation of HSP27 phosphorylation was confirmed through use of hyoscyamine, the active enantiomer of atropine. Preincubation of SH-SY5Y cells for 60 min with a 1 μM concentration of this muscarinic receptor antagonist had no significant effect on basal phosphorylation of HSP27, but reduced CCh-stimulated phosphorylation to a level that was not significantly different from basal values (Fig. 2A). Incubation with 1 mM nicotine for 1 or 5 min had no stimulatory effect on HSP27

phosphorylation. Specificity of the CCh effect was indicated since bradykinin, another agonist that activates $G_{q/11}$-coupled receptors on SH-SY5Y cells (Rosethorne et al., 2008) also did not increase HSP27 phosphorylation significantly above basal levels (Fig. 2B).

3.2 Involvement of p38 MAPK and PKC in HSP27 phosphorylation

Activation of the p38 MAPK/MAPKAPK-2 pathway is a well-characterized mechanism for the phosphorylation of HSP27 at Ser-82. In addition, PKC, which is activated by $G_{q/11}$-coupled receptors, phosphorylates HSP27 at this site either directly or through p38 MAPK and/or PKD (Kostenko and Moens, 2009). Therefore, the effects of inhibitors of these protein kinases on the phosphorylation of HSP27 were determined in SH-SY5Y cells (Fig. 3A). Note that in these and all other experiments that used protein kinase inhibitors, concentrations of these compounds were chosen with careful attention to the literature so as to achieve selective inhibition of the target protein kinase in cultured cells (Table I). Cells were preincubated with the p38 MAPK inhibitor, SB 203580 (10 μM), or the PKC inhibitor, GF 109203X (5 μM) for 60 min prior to the addition of CCh for 5 min. Neither inhibitor had a significant effect on basal HSP27 phosphorylation, alone or in combination. Preincubation with either SB 203580 or GF 109203X had small inhibitory effects on CCh-stimulated phosphorylation of HSP27 at Ser-82. When the two protein kinase inhibitors were combined, in the presence of CCh they produced an additive and statistically significant inhibition of HSP27 phosphorylation, although not to basal levels.

Lack of a prominent involvement of p38 MAPK or PKC in CCh-mediated HSP27 phosphorylation was in contrast to its phosphorylation in response to other stimuli. When SH-SY5Y cells were incubated with the phorbol ester, PDB, a known activator of PKC, at a concentration of 1 μM for 15 min, HSP27 phosphorylation was completely sensitive to GF 109203X (Fig. 3B). Hyperosmotic stress is the prototypical stimulus that activates the p38MAPK/MAPKAPK-2 pathway (Sheik-hamad and Gustin, 2004). Exposure of SH-SY5Y cells to hyperosmotic conditions, produced by addition of 0.3M sorbitol to the incubation medium for 30 min, elicited increased phosphorylation of HSP27 that was nearly completely reversed by the p38 MAPK inhibitor, SB 203580. These positive controls indicate that the protein kinase inhibitors were active against appropriate kinase targets at the concentrations employed in the experiments with CCh. In a more general sense, they demonstrate that HSP27 phosphorylation at Ser-82 is sensitive to multiple stimuli.

3.3 Comparison of muscarinic receptor-and PDB-mediated HSP27 phosphorylation

Since CCh stimulates phosphorylation of HSP27 through muscarinic receptors coupled to multiple protein kinases while PDB directly activates only PKC, it was of interest to compare these stimuli with regard to the properties of HSP27 phosphorylation. Analysis of HSP27 phosphorylation was extended to include the three major phosphorylation sites in this protein. SH-SY5Y cells were incubated with either CCh or PDB, after which cell lysates were prepared and immunoblotted with phospho-specific antibodies to Ser-15, Ser-78 and Ser-82. When normalized to the amount of total HSP27 in lysates, different patterns of phosphorylation were seen in response to the two stimuli (Fig. 4A): CCh increased phosphorylation at Ser-78 and Ser-82 to an equal extent while PDB was effective only in stimulating phosphorylation of Ser-82. Neither CCh nor PDB increased the phosphorylation of Ser-15 (Fig. 4B).

Although the sole action of a phorbol ester such as PDB is the activation of PKC, both p38 MAPK and/or PKD are reported to be downstream intermediates of PKC signaling in the phosphorylation of HSP27 at Ser-82 (Takai et al, 2007; Yuan and Rozengurt, 2008). Therefore, the abilities of a p38 MAPK inhibitor (SB 203580) and a PKD inhibitor (CID 755673) to inhibit PDB-induced phosphorylation of HSP27 were compared. As shown in

Fig. 4C, the former had no effect on stimulation of HSP27 phosphorylation produced by 1 μM PDB. Incubation of cells with CID 755673, however, inhibited the effect of PDB to an extent equal to that produced by inhibition of PKC with GF 109203X. CID 755673 had no effect on basal HSP27 phosphorylation (data not shown). Thus, the predominant pathway mediating PDB-induced phosphorylation of HSP27 at Ser-82 in SH-SY5Y cells appears to be from PKC through PKD.

3.4 The PI3-K pathway modulates HSP27 phosphorylation

Since the combination of GF 109203X and SB 203580 only reduced CCh-stimulated HSP27 phosphorylation by approximately 50%, the involvement of an additional protein kinase is implied. Since exposure of SH-SY5Y cells to CCh increased the phosphorylation of ERK1/2 and Akt at sites linked to activation of these protein kinases (Figs. 5A and B), the effects of inhibitors of the ERK1/2 and PI3-K pathways on muscarinic receptor-mediated phosphorylation of HSP27 were compared. The MAP kinase kinase (MKK) inhibitor, PD 98059, did not alter CCh-stimulated HSP27 phosphorylation at 10 μM (Fig. 5C), a concentration that blocks insulinlike growth factor-1-dependent phosphorylation of ERK2 and neurite outgrowth in SH-SY5Y cells (Kim et al., 1997). The involvement of ERK1/2 in HSP27 phosphorylation was therefore eliminated from further consideration in this study. In contrast, the PI3-K pathway was related to muscarinic receptor-activated HSP27 phosphorylation in a complex manner.

Cells were incubated with inhibitors of three major protein kinases that are sequential components of the PI3-K pathway: LY 294002 (PI3-K), Akti-1/2 (Akt isoforms 1 and 2), and rapamycin, [mammalian target of rapamycin complex (mTORC)1]. The expectation was that if any of these protein kinases were involved in phosphorylation of HSP27 at Ser-82, the respective inhibitor of that enzyme would block the effect of CCh. Paradoxically, 60 min of incubation with 50 μM LY 294002 or 10 μM Akti-1/2 significantly increased HSP27 phosphorylation (Fig. 6A). Both basal and CCh-stimulated phosphorylation were affected by LY 294002 while Akti-1/2 stimulated only basal phosphorylation. Rapamycin, which acts on mTORC1 downstream of Akt, had no stimulatory effect on basal HSP27 phosphorylation and produced only a small, insignificant reduction in CCh-stimulated phosphorylation. The activity of LY 294002, Akti-1/2 or rapamycin was confirmed by the inhibition of CCh-stimulated Akt or S6 ribosomal protein phosphorylation in cell lysates (Fig. 6B). Akt is a downstream target of PI3-K while Akti-1/2 prevents a conformational change in Akt that allows its phosphorylation by PDK1 and mTORC2 (Bain et al., 2007). The S6 ribosomal protein is a substrate of mTORC1.

These results being consistent with a relationship between Akt and HSP27, a more detailed analysis of the effect of Akti-1/2 on HSP27 phosphorylation was performed (Fig. 6C). Akti-1/2-mediated increases in HSP27 phosphorylation were blocked by simultaneous incubation with SB 203580, implying an inverse relationship between Akt and p38 MAPK activities. Support for this relationship was provided by increased phosphorylation of p38 MAPK at Thr-180/Tyr-182, a site that determines p38 MAPK activity, in cell lysates prepared from cells following incubation with Akti-1/2 (Fig. 6D). Under the same conditions, CCh produced only a small, insignificant increase in p38 MAPK phosphorylation, consistent with the relatively small effect of the p38 MAPK inhibitor, SB 203580, on HSP27 phosphorylation at Ser-82 (Fig. 3A). When Akti-1/2 was combined with GF 109203X, phosphorylation was not different from that produced by preincubation with Akti-1/2 alone (Fig. 6C). Since the combination of SB 203580, GF 109203X and Akti-1/2 reduced HSP27 phosphorylation to basal levels ± CCh, muscarinic receptor-mediated phosphorylation of HSP27 at Ser-82 can be totally accounted for by PKC, p38MAPK and Akt. These results also demonstrate that the degree to which Ser-82 in HSP27 is

phosphorylated by p38 MAPK after muscarinic receptor activation can be modulated through the PI3-K pathway, presumably by interactions of p38 MAPK with Akt.

3.5 HSP27 phosphorylation in differentiated SH-SY5Y cells

Even though the SH-SY5Y cell line is commonly taken to be a model for neurons, there are inherent limitations in using an undifferentiated neuroblastoma to examine neuronal processes. To increase the physiological relevance of this study, it was determined whether differentiated SH-SY5Y cells respond to the three modulators that increase HSP27 phosphorylation in undifferentiated cells: CCh, PDB and Akti-1/2. To achieve this, SH-SY5Y cells were differentiated in serum-free medium containing a low concentration of PDB and a growth factor, in this case, bFGF. These conditions produce a mature neuronal phenotype including expression of specific protein markers, catecholaminergic properties and elaboration of a network of processes with varicosities and growth cones (Lavenius et al, 1994; Pahlman et al, 1995).

After 5 days of culture in serum-free medium containing 16 nM PDB and 3 nM bFGF, SH-SY5Y cells display much longer processes than undifferentiated cells grown for 2 days in DMEM with 10% FBS, the standard conditions used to analyze HSP27 phosphorylation (Fig. 7A and B). Cells cultured for the same time in serum-free medium alone resemble the latter with the short, pointed processes characteristic of SH-SY5Y cells. (data not shown). As described in the original report of the differentiation protocol (Lavenius et al, 1994), some of the processes contain varicosities and terminate in growth-cone-like structures. Following differentiation, SH-SY5Y cells respond acutely to 1 μM PDB with a GF 109203X–sensitive phosphorylation of HSP27 that is comparable to that seen in undifferentiated cells, indicating that PKC has not been down-regulated during the 5 day exposure to nM concentrations of PDB (Fig. 7C). Increased phosphorylation of HSP27 also occurs in differentiated cells in response to CCh or Akti-1/2. The magnitude of these effects appears to be less than obtained in the undifferentiated cells, however, the pharmacological sensitivity of the CCh-mediated increase to hyoscyamine demonstrates that muscarinic receptors are still coupled to HSP27 phosphorylation in differentiated cells. In addition, reversal of Akti-1/2-mediated HSP27 phosphorylation by SB 203580 replicates the inverse relationship between Akt and p38 MAPK that is seen in undifferentiated cells (Fig. 7C).

3.6 Immunolocalization of phosphorylated HSP27 and f-actin in response to CCh and PDB

Phosphorylation of HSP27 is functionally associated with remodeling of the actin cytoskeleton and alterations in cell morphology (Gusev, et al., 2002; Mounier and Arrigo, 2002; During et al., 2007), both of which are also modulated in SH-SY5Y cells by muscarinic receptor activation or exposure to a phorbol ester (Rösner et al., 1995; Danks et al., 1999). Given the different pathways leading to phosphorylation of HSP27 in response to CCh-mediated muscarinic receptor activation and the phorbol ester, PDB, phase contrast microscopy and immunofluorescence microscopy were used to compare changes in the organization of the actin-based cytoskeleton that occur when HSP27 phosphorylation at Ser-82 is modulated in (undifferentiated) SH-SY5Y cells by either stimulus. In control cells, phospho-HSP27 immunolabeling had a finely dispersed, speckled distribution (Fig. 8A). When preimmuune rabbit IgG was substituted for a primary antibody directed against phospho-HSP27, little to no immunostaining was observed (data not shown). Following stimulation of muscarinic receptors with 1 mM CCh for 5 min, phospho-HSP27 (Ser-82) immunostaining became generally more intense but with a dispersed, punctuate or reticulated appearance at the cell margins and denser perinuclear immunostaining (Fig. 8D). Similar changes in phospho-HSP27 level and distribution occurred when cells were stimulated for 15 min with 1 μM PDB (Fig. 8G). Thus, although CCh and PDB stimulate

phosphorylation of Ser-82 in HSP27 through different combinations of protein kinases, the pattern of immunostaining in response to either stimulus is comparable.

In control cells, f-actin, as visualized with rhodamine-phalloidin, was principally seen as fibers but with some intense spots that may be focal adhesions (Fig. 8B). Exposure to 1 mM CCh for 5 min produced a modest increase in actin filaments associated with some broadening of the short cell processes (Fig. 8E). In contrast, 15 min of stimulation with 1 μM PDB caused extensive re-organization of the f-actin cytoskeleton into arrays of filaments at the margins of elaborate lamellipodial processes (Fig. 8H). Overlay of labeled f-actin and phospho-HSP27 images demonstrates segregation of these two proteins at such PDB-induced sites (Fig 8I) in comparison to either the control or CCh condition (Fig. 8C and F). The differences in CCh- and PDB-induced HSP27 immunfluorescence relative to the actin cytoskeleton at cell processes are most readily observed in microscopic fields containing a single cell as in the representative double-labeled examples shown in the lower panel of Fig. 8.

Since the phosphorylation of HSP27 in response to PDB can be attributed to the activation of a single protein kinase pathway (PKC to PKD), this stimulus was chosen to examine morphological changes that may reflect interaction between phosphorylated HSP27 and f-actin. The morphology of undifferentiated cells was examined after 15 min or 2 hr of exposure to PDB. In the latter case, the concentration of PDB was reduced from 1 μM to 10 nM to avoid down-regulation of PKC over the longer time period. Immunoblotting following 2 hr of exposure of cells to 10 nM PDB confirmed that HSP27 is phosphorylated at Ser-82 to an equal extent as obtained with 1 μM PDB for 15 min (data not shown). The more acute set of conditions was chosen to correspond to those used to produce rapid changes in HSP27 phosphorylation. The second allowed assessment of the duration of morphological effects in relation to HSP27 phosphorylation since 10 nM PDB induces changes in SH-SY5Y cell morphology starting at 10 min of exposure that are maintained for up to 24 hr (Rösner et al., 1995).

Acute treatment with 1 μM PDB for 15 min caused rapid elaboration of lamellipodial processes at the ends of the short, pointed processes normally observed on cells and extensive remodeling at the cell margins (Figs. 9A–C). These changes were persistent as identical cellular phenotypes were observed after exposure of cells to 10 nM PDB for 2 hr (Figs. 9D–F). Involvement of PKC was demonstrated through blockade of the morphological change by preincubation of cells with 5 μM GF 109203X prior to addition of PDB. In contrast to the lamellipodial profile of PDB-treated cells, GF 109203X, either alone or in combination with PDB treatment, caused elongation and secondary branching of filopodial processes (Fig. 10A; Compare Figs. 10B and C). Thus, inhibition and stimulation of PKC have opposing effects on SH-SY5Y cell morphology.

To obtain a more quantitative measure of the morphology changes and to compare the effects of PKC or PKD inhibition on formation of lamellipodia, cells were incubated with PDB following preincubation with or without GF 109203X or CID 755673 after which fields of cells were counted for the presence of flared lamellipodia. The results of this analysis are shown in Table II. In response to PDB, approximately 45% of the cells in any one field have flared lamellipodia. This phenotype was rarely observed in control cells or in the presence of either protein kinase inhibitor alone. Preincubation of cells with GF 109203X completely blocked the reorganization into lamellipodial profiles by PDB. In contrast, inhibition of PKD with CID 755673 was without effect on PDB-induced lamellipodia.

4. Discussion

HSP27 acts to protect cells, including neurons, from injurious stimuli, whether it is constitutively expressed (Lewis et al., 1999) or following induction by heat shock or experimental manipulations (Akbar et al., 2003; Dodge et al., 2006; Sharp et al., 2008). This overall function occurs in a pleiotropic manner through inhibition of apoptosis, chaperoning of misfolded proteins, activation of the proteasome and stabilization of the actin cytoskeleton (Arrigo, 2007). The chaperone function of HSP27 is mediated by its dephosphorylated oligomeric form (Lambert et al., 1999; Rogalla et al., 1999) while phosphorylation-dependent disassociation of HSP27 oligomers is required to block apoptosis (Gusev et al., 2002; Benn and Woolf, 2004). Moreover, the way in which HSP27 interacts with actin differs based on its phosphorylation state (Mounier and Arrigo, 2002). Therefore, it is of interest to characterize mechanisms that regulate the multiple protein kinases that phosphorylate HSP27.

4.1 Significance of muscarinic receptor-mediated phosphorylation of HSP27

HSP27 is documented in the literature as a neuroprotective protein, promoting survival and chaperoning proteins that aggregate in neurodegenerative states (Benn and Woolf, 2004; Klettner, 2004; Latchman, 2005; Koren et al., 2009). Since HSP27 phosphorylation is an obligate determinant of its functions, it is desirable to stimulate this posttranslational modification without resorting to stressful conditions such as heat shock or exposure to toxic agents. This first characterization of HSP27 phosphorylation in response to muscarinic receptor activation in a cell with a neuron-like phenotype suggests that synaptic cholinergic receptor-mediated signaling could provide a means to do so given adequate expression of HSP27.

Most neurons do not contain appreciable levels of HSP27 under basal conditions, sensory neurons and limited populations in the CNS being notable exceptions. However, in response to insult or pathology, neuronal HSP27 expression is up-regulated in a more generalized way (Akbar et al., 2001; 2003). Thus, under conditions when activation of the functions of HSP27 would be most beneficial, muscarinic receptor-mediated phosphorylation might be an effective means to achieve this. SH-SY5Y cells differentiated with a phorbol ester and growth factor are phenotypically similar to dopaminergic neurons and have the potential to model aspects of the neurochemistry of Parkinson's disease (Reviewed by Xie et al, 2010). Such differentiated cells retain cholinergic receptors (Pahlman et al., 1995) and our observation that they respond to CCh with increased HSP27 phosphorylation in a hyoscyamine-sensitive manner indicates their potential to test the hypothesis that muscarinic receptor-mediated phosphorylation serves an adaptive purpose in neurons.

4.2 PKC Signaling and HSP27 phosphorylation

Given activation of phospholipase Cβ by $G_{q/11}$-coupled muscarinic receptors, it would be expected that CCh binding to the M_3 receptor increases PKC activity through generation of 1, 2-diacylglycerol. Indeed, in SH-SY5Y cells, CCh-stimulated HSP27 phosphorylation is partially sensitive to GF 109203X, an inhibitor of PKC, while direct stimulation of PKC with a phorbol ester produces significant phosphorylation of HSP27 at Ser-82. Recently, PKD, a member of the calcium/calmodulin-dependent protein kinase family that is activated by PKC-dependent phosphorylation, was demonstrated to be a HSP27 kinase in pancreatic cancer cells (Yuan and Rozengurt, 2008). In this instance and others, p38 MAPK-mediated phosphorylation of HSP27 was also secondary to PKC activation (Nomura et al., 2007; Guo et al., 2008). However, the inability of a p38 MAPK inhibitor to affect phorbol ester-stimulated HSP27 phosphorylation eliminates this possibility in SH-SY5Y cells. Conversely, the complete reduction of HSP27 phosphorylation produced by inhibitors of

either PKC or PKD indicates that all of the phosphorylation of HSP27 that is induced by a phorbol ester occurs through this pathway.

Activation of PKC by PDB is a more selective stimulus than muscarinic receptor activation not only because the subsequent phosphorylation of HSP27 occurs through a single kinase pathway, but also because only one of the three phosphorylation sites in HSP27 (Ser-82) is modified. In contrast, CCh increases phosphorylation comparably at both Ser-78 and Ser-82. The resultant double negative charge at two amino acids residues close to one another is likely to uniquely determine interactions of HSP27, both with itself in oligomers and with other proteins.

4.3 The PI3-K pathway and HSP27 phosphorylation

The combination of p38 MAPK and PKC inhibitors did not return CCh-stimulated HSP27 phosphorylation to basal levels indicating that there was another protein kinase involved. The possibility that this was Akt was considered since there is an association between HSP27 and Akt, both as a physical complex (Zheng et al. 2006) and in functional terms during adaptation to stressors or NGF withdrawal (Konishi et al., 1997; Mearow et al., 2002). Also, this study and others (Tang et al., 2002; Anger et al., 2007) have demonstrated that Akt phosphorylation at Ser-473 increases when M_3 muscarinic receptors are stimulated with CCh.

As a first approach to establish a relationship between the PI3-K pathway and HSP27 phosphorylation, SH-SY5Y cells were incubated with inhibitors of three sequential protein kinases in this pathway, PI3-K, Akt and mTORC1. Unexpectedly, inhibition of either PI3-K or Akt stimulated basal phosphorylation of HSP27 and the PI3-K inhibitor, LY 294002, also increased CCh-mediated stimulation of HSP27 phosphorylation. An inverse relationship between the PI3-K and p38 MAPK pathways accounted for this effect since 1.) simultaneous incubation of Akti-1/2 and SB 203580 completely blocked such stimulation, and 2.) the phosphorylation of p38 MAPK at Thr-180/Tyr-182, a marker of its activation, was increased when Akt was inhibited.

Phosphorylation of effector proteins by mTORC1 occurs following M_3 receptor activation; notably, mTORC1-mediated S6 phosphorylation is stimulated by CCh in SK-N-SH neuroblastoma cells without a change in Akt phosphorylation (Slack and Blusztajn, 2008). Therefore, the possibility that HSP27 might be a substrate of mTORC1 was addressed through use of the selective inhibitor of this protein kinase, rapamycin. Rapamycin produced no stimulation of basal HSP27 phosphorylation and did not affect CCh-stimulated phosphorylation. Thus, the focal point for reciprocal regulation of PI3-K and p38 MAPK in SH-SY5Y cells appears to be at the level of Akt.

The p38MAPK pathway is primarily involved in stress-activated phosphorylation of HSP27 (Rouse et al., 1994). It is not directly coupled to muscarinic receptors in SH-SY5Y cells since the selective p38 MAPK inhibitor, SB 203580, has only a small partial effect on CCh-stimulated phosphorylation of Ser-82 in HSP27. However, the inverse relationship that exists between Akt and p38 MAPK (i.e., p38 MAPK activity fully accounts for HSP27 phosphorylation at Ser-82 when Akt is inhibited) is consistent with a role in stress-activated signaling. Because Akt is involved in survival pathways in neuroblastoma (Li and Thiele, 2007), its inhibition could represent a stressor that switches HSP27 phosphorylation to p38 MAPK as an adaptive response.

4.4 HSP27 phosphorylation in relation to cytoskeletal organization

Phosphorylation of HSP27 is linked to alterations in the actin-based cytoskeleton within several contexts. Resistance to heat shock is dependent upon HSP27 phosphorylation with

resultant cytoskeletal stability (Lavoie et al., 1995; Geum et al., 2002). Interaction of phosphorylated HSP27 with the actin cytoskeleton is not strictly a correlate of the stressed state, however, as it also mediates mitogenic stimulation and cell motility (Lavoie et al., 1993; Nomura et al., 2007). Such an association has pathological relevance since anthrax lethal toxin paralyzes neutrophils, which are responsible for innate immunity, by blocking HSP27 phosphorylation and actin-based motility (During et al., 2007). Muscarinic receptor activation and phorbol ester induce a phenotype in SH-SY5Y cells that includes formation of lamellipodial protrusions and movement of dense-cored vesicles to the plasma membrane for secretion of catecholamine, processes that require reorganization of the actin cytoskeleton (Rösner et al., 1995; Viviani et al., 1996; Danks et al., 1999).

For these reasons, we have investigated relationship(s) between HSP27 phosphorylation, actin reorganization and morphology in SH-SY5Y cells. Both CCh and PDB similarly increase phospho-HSP27 immunofluorescence and alter cellular distribution of phosphorylated HSP27 in SH-SY5Y cells to a perinuclear localization that is typical of its activated state. Stimulation of cells also produces regions near the cell margins where phospho-HSP27 immunofluorescence becomes more dispersed or reticular in appearance. We have emphasized the phorbol ester-induced HSP27 phosphorylation in relation to the state of f-actin and resultant changes in cell morphology since it can be related completely to the PKC/PKD pathway.

Three aspects of our results indicate that PKC/PKD-mediated phosphorylation of HSP27 at Ser-82 is not a major factor during actin reorganization in SH-SY5Y cells. Firstly, the lamellipodia formation that results from actin reorganization in response to PDB is not sensitive to inhibition of PKD although an inhibitor of PKC completely blocks it. This is in opposition to HSP27 phosphorylation at Ser-82 that is entirely sensitive to inhibition of either kinase. Secondly, in our system, phosphorylated HSP27 clearly segregates from the actin filaments that form at lamellipodial margins in response to phorbol ester eliminating a model in which phosphorylated monomers of HSP27 directly associate with filamentous actin (Lavoie et el., 1995; Rogalla et al., 1999). It is possible that HSP27 more subtly modulates actin reorganization through another mechanism. For example, dephosphorylated HSP27 may be either a barbed end capping protein (Benndorf et al., 1994) or sequester free G-actin monomers (During et al. 2007). In either case, actin polymerization would be prohibited while phosphorylation of HSP27 would allow remodeling of the cytoskeleton to proceed. However, PDB and CCh produce similar changes in phosphorylation and cellular distribution of HSP27 while only the former strongly induces lamellipodial formation. This argues against such models and implies that downstream targets of PKC other than PKD and phospho(Ser-82)-HSP27 are more critical in this regard. Our results differ from what is observed in glioblastoma cells, where phorbol ester-induced HSP27 phosphorylation depends upon the p38 MAPK/MAPKAPK-2 pathway and phospho-HSP27 does co-localize with f-actin (Nomura et al., 2007). Thus, the signal transduction mechanisms that regulate HSP27 phosphorylation appear to be quite cell-specific, even among malignant cells that are characterized by a high degree of motility and abundant expression of HSP27 (Calderwood and Ciocca, 2008).

Finally, given that muscarinic receptor-mediated HSP27 phosphorylation is via multiple protein kinases, functions other than PKC-mediated regulation of f-actin structure are likely be of significance in SH-SY5Y cells. Given the rapid maximal increase in HSP27 phosphorylation that occurs in response to CCh, these are likely to be acute processes. One possibility is catecholamine release which is stimulated by both muscarinic receptor activation and phorbol ester over a short time course in these cells (Rösner et al., 1995; Viviani et al., 1996; Danks et al., 1999).

Abbreviations

Akti-1/2	1,3-Dihydro-1-(1-((4-(6-phenyl-1H–imidazo[4,5-*g*]quinoxalin-7-yl)phenyl)methyl)-4-piperidinyl)-2H–benzimidazol-2-one
bFGF2	Basic fibroblast growth factor
CCh	Carbamoylcholine chloride (carbachol)
CID 755673	2,3,4,5-Tetrahydro-7-hydroxy-1*H*–benzofuro[2,3-*c*]azepin-1-one
DAPI	4’,6-diamidino-2-phenylindole
DMEM	Dulbecco’s Modification of Eagle’s Medium
ERK	Extracellular stimulus-regulated protein kinase
FBS	Fetal bovine serum
GF 109203X	2-[1-(3-Dimethylaminopropyl)-1H–indol-3-yl]-3-(1H–indol-3-yl)-maleimide
HSP27	Heat shock protein 27
IGF-1	Insulin-like growth factor-1
IgG	Immunoglobulin fraction G
LY 294002	2-(4-Morpholinyl)-8-phenyl-4H-1-benzopyran-4-one
MAPK	Mitogen-activated protein kinase
MAPKAPK-2	MAPK-activated protein kinase-2
PD 98059	2-Amino-3’-methoxyflavone
PDB	Phorbol-12, 13-dibutyrate
MKK	MAP kinase kinase
mTORC	Mammalian target of rapamycin complex
PI3-K	Phosphatidylinositol 3-kinase
PLB	Passive lysis buffer
PKC	Protein kinase C
PVDF	Polyvinylidene fluoride
SB 203580	4-(4-Fluorophenyl)-2-(4-methylsulfinylphenyl)-5-(4-pyridyl)1H–imidazole
SDS-PAGE	Sodium dodecylsulfate polyacrylamide gel electrophoresis

Acknowledgments

This research was supported by NIH Grants NS31173 (W.S.M.), DK080640 (S.M.N.), GM085756 (F.E.W.) and a grant from the Center for Successful Aging at The University of Toledo (L.A.D.). Dr. William Messer holds several patents on muscarinic agonists. He is the Chief Scientific Officer for and has financial interest in Mithridion, Inc., Madison, WI/Toledo, OH. Shantanu Rao is thanked for his assistance with maintenance of cell cultures. Drs. Huda Akil and Stanley Watson of the University of Michigan, Ann Arbor MI, kindly provided laboratory facilities for experiments done during the revision of this manuscript.

References

Akbar MT, Wells DJ, Latchman DS, deBelleroche J. Heat shock protein 27 shows a distinctive widespread spatial and temporal pattern of induction in CNS glial and neuronal cells compared to

heat shock protein 70 and caspase 3 following kainate administration. Mol. Brain Res. 2001; 93:148–163. [PubMed: 11589992]

Akbar MT, Lundberg AM, Liu K, Vidyadaran S, Wells KE, Dolatshad H, Wynn S, Wells DJ, Latchman DS, deBellroche J. The neuroprotective effects of heat shock protein 27 overexpression in transgenic animals against kainate-induced seizures and hippocampal cell death. J. Biol. Chem. 2003; 278:19956–19965. [PubMed: 12639970]

Anger T, Klintworth N, Stumpf C, Daniel WG, Mende U, Garlichs CD. RGS protein specificity towards G_q- and $G_{i/o}$-mediated ERK1/2 and Akt activation *in vitro*. J. Biochem. Mol. Biol. 2007; 40:899–910. [PubMed: 18047785]

Arrigo AP. The cellular "networking" of mammalian Hsp27 and its functions in the control of protein folding, redox and apoptosis. Adv. Exp. Med. Biol. 2007; 594:14–26. [PubMed: 17205671]

Badin RA, Lythgoe MF, van der Weerd L, Thomas DL, Gadian DG, Latchman DS. Neuroprotective effects of virally delivered HSPs in experimental stroke. J. Cereb. Blood Flow Metab. 2006; 26:371–381. [PubMed: 16079790]

Bain J, Plater L, Elliot M, Shapiro N, Hastie CJ, McLauchlan H, Klevernic I, Arthur JS, Alessi DR, Cohen P. The selectivity of protein kinase inhibitors: A further update. Biochem. J. 2007; 408:297–315. [PubMed: 17850214]

Barnett SF, Defeo-Jones D, Fu S, Hancock PJ, Haskell KM, Jones RE, Kahana JA, Kral AM, Leander K, Lee LL, Malinowski J, McAvoy EM, Nahas DD, Robinson RG, Huber HE. Identification and characterization of pleckstrin-homology-domain-dependent and isozyme-specific Akt inhibitors. Biochem. J. 2005; 385:399–408. [PubMed: 15456405]

Bechtold DA, Brown IR. Induction of Hsp27 and Hsp32 stress proteins and vimentin in glial cells of the rat hippocampus following hyperthermia. Neurochem. Res. 2003; 28:1163–1173. [PubMed: 12834255]

Benn SC, Perrelet D, Kato AC, Scholz J, Decosterd I, Mannion RJ, Bakowska JC, Woolf CJ. Hsp27 upregulation and phosphorylation is required for injured sensory and motor neuron survival. Neuron. 2002; 36:45–56. [PubMed: 12367505]

Benn SC, Woolf CJ. Adult neuron survival strategies - slamming on the brakes. Nature Rev. Neurosci. 2004; 5:686–700. [PubMed: 15322527]

Benndorf R, Hayess K, Ryazantsev S, Wieske M, Behlke J, Lutsch G. Phosphorylation and supramolecular organization of murine small heat shock protein HSP25 abolish its actin polymerization-inhibiting activity. J. Biol. Chem. 1994; 269:20780–20784. [PubMed: 8051180]

Calderwood SK, Ciocca DR. Heat shock proteins: stress proteins with Janus-like properties in cancer. Int. J. Hypothermia. 2008; 24:31–39.

Chen S, Brown IR. Neuronal expression of constitutive heat shock proteins: implications for neurodegenerative diseases. Cell Stress Chaperones. 2007; 12:51–58. [PubMed: 17441507]

Cuenda A, Rouse J, Doza YN, Meier R, Cohen P, Gallagher TF, Young PR, Lee JC. SB 203580 is a specific inhibitor of a MAP kinase homologue which is stimulated by cellular stresses and interleukin-1. FEBS Lett. 1995; 364:229–233. [PubMed: 7750577]

Danks K, Wade JA, Batten TFC, Walker JH, Ball SG, Vaughn PFT. Redistribution of F-actin and large dense-cored vesicles in the human neuroblastoma SH-SY5Y in response to secretagogues and protein kinase Cα activation. Mol. Brain. Res. 1999; 64:236–245. [PubMed: 9931495]

Davies SP, Reddy H, Caivano M, Cohen P. Specificity and mechanism of action of some commonly used protein kinase inhibitors. Biochem. J. 2000; 351:95–105. [PubMed: 10998351]

DeSarno P, Shestopal SA, King TD, Zmijewska A, Song L, Jope R. Muscarinic receptor activation protects cells from apoptotic effects of DNA damage, oxidative stress, and mitochondrial inhibition. J. Biol. Chem. 2003; 278:11086–11093. [PubMed: 12538580]

Dodge ME, Wang J, Guy C, Rankin S, Rahimtula M, Mearow KM. Stress-induced heat shock protein 27 expression and its role in dorsal root ganglion neuronal survival. Brain Res. 2006; 1068:34–46. [PubMed: 16376863]

During RL, Gibson BG, Li W, Bishai EA, Sidhu GS, Landry J, Southwick FS. Anthrax lethal toxin paralyzes actin-based motility by blocking Hsp27 phosphorylation. The EMBO J. 2007; 26:2240–2250.

Geum D, Son GH, Kim K. Phosphorylation-dependent cellular localization and thermoprotective role of heat shock protein 25 in hippocampal progenitor cells. J. Biol. Chem. 2002; 277:19913–19921. [PubMed: 11912188]

Gerthoffer WT. Actin cytoskeletal dynamics in smooth muscle contraction. Can. J. Physiol. Pharmacol. 2005; 83:851–856. [PubMed: 16333356]

Guo K, Liu Y, Zhou H, Dai Z, Zhang J, Sun R, Chen J, Sun Q, Lu W, Kang X, Chen P. Involvement of protein kinase Cβ-extracellular signal-regulating kinase1/2/p38 mitogen-activated protein kinase-heat shock protein 27 activation in hepatocellular carcinoma cell motility and invasion. Cancer Sci. 2008; 99:486–496. [PubMed: 18167130]

Gusev NB, Bogatcheva NV, Marston SB. Structure and properties of small heat shock proteins (sHsp) and their interaction with cytoskeletal proteins. Biochem. (Moscow). 2002; 67:613–623.

Heikkilä J, Jalava A, Eriksson K. The selective protein kinase C inhibitor GF 109203X inhibits phorbol ester-induced morphological and functional differentiation of SH-SY5Y human neuroblastoma cells. Biochem. Biophys. Res. Comm. 1993; 197:1185–1193. [PubMed: 8280132]

Kim B, Leventhal PS, Saltiel AS, Feldman EL. Insulin-like growth factor-I-mediated neurite outgrowth *in vitro* requires mitogen-activated protein kinase activation. J. Biol. Chem. 1997; 272:21268–21273. [PubMed: 9261137]

King M, Naffar F, Clarke J, Mearow K. The small heat shock protein Hsp27 protects cortical neurons against the toxic effects of beta-amyloid peptide. J. Neurosci. Res. 2009; 87:3161–3175. [PubMed: 19530165]

Klettner A. The induction of heat shock proteins as a potential strategy to treat neurodegenerative disorders. Drug News Perspect. 2004; 17:299–306. [PubMed: 15334179]

Konishi H, Matsuzaki H, Tanaka M, Takemura Y, Kuroda S, Ono Y, Kikkawa U. Activation of protein kinase B (Akt/RAC-protein kinase) by cellular stress and its association with heat shock protein Hsp27. FEBS Lett. 1997; 410:493–498. [PubMed: 9237690]

Koren J 3rd, Jinwal UK, Jones JR, Shults CL, Johnson AJ, Anderson LJ, Dickey CA. Chaperone signaling complexes in Alzheimer's disease. J. Cell Mol. Med. 2009; 13:19–30.

Kostenko S, Moens U. Heat shock protein 27 phosphorylation: kinases, phosphatases, functions and pathology. Cell. Mol. Life Sci. 2009; 66:3289–3307. [PubMed: 19593530]

Lambert DG, Ghataorre AS, Nahorski SR. Muscarinic receptor binding characteristics of a human neuroblastoma SK-N-SH and its clones SH-SY5Y and SH-EP1. Eur. J. Pharmacol. 1989; 165:71–77. [PubMed: 2767136]

Lambert H, Charette SSJ, Bernier AF, Guimond A, Landry J. HSP27 multimerization mediated by phosphorylation-sensitive intermolecular interactions at the amino terminus. J. Biol. Chem. 1999; 274:9378–9385. [PubMed: 10092617]

Landry J, Huot J. Regulation of actin dynamics by stress-activated protein kinase 2 (SAPK2)-dependent phosphorylation of heat-shock protein of 27 kDa (Hsp27). Biochem. Soc. Symp. 1999; 64:79–89. [PubMed: 10207622]

Latchman DS. HSP27 and cell survival in neurons. Int. J. Hyperthermia. 2005; 21:393–402. [PubMed: 16048837]

Lavenius E, Parrow V, Nanberg E, Pahlman S. Basic FGF and IGF-1 promote differentiation of human SH-SY5Y neuroblastoma cells in culture. Growth Factors. 1994; 10:29–39. [PubMed: 7514011]

Lavioe JN, Hickey E, Weber LA, Landry J. Modulation of actin microfilament dynamics and fluid phase pinocytosis by phosphorylation of heat shock protein 27. J. Biol. Chem. 1993; 268:24210–24214. [PubMed: 8226968]

Lavoie JN, Lambert H, Hickey E, Weber LA, Landry J. Modulation of cellular thermoresistance and actin filament stability accompanies phosphorylation-induced changes in the oligomeric structure of heat shock protein 27. Mol. and Cell. Biol. 1995; 15:505–516. [PubMed: 7799959]

Lewis SE, Mannion RJ, White FA, Coggeshall RE, Beggs S, Costigan M, Martin JL, Dillman WH, Woolf CJ. A role for HSP27 in sensory neuron survival. J. Neurosci. 1999; 19:8945–8953. [PubMed: 10516313]

Li Z, Thiele CJ. Targeting Akt to increase the sensitivity of neuroblastoma to chemotherapy: lessons learned from the brain-derived neurotrophic factor/TrkB signal transduction pathway. Expert. Opin. Ther. Targets. 2007; 11:1611–1621. [PubMed: 18020981]

Mearow KM, Dodge ME, Rahimtula M, Yegappan C. Stress-mediated signaling in PC12 cells-the role of the small heat shock protein, Hsp27, and Akt in protecting cells from heat stress and nerve growth factor withdrawal. J. Neurochem. 2002; 83:452–462. [PubMed: 12423255]

Mookherjee P, Quintanilla R, Roh MS, Zmijewski AA, Jope RS, Johnson GV. Mitochondrial-targeted active Akt protects SH-SY5Y neuroblastoma cells from staurosporine-induced apoptotic cell death. J. Cell. Biochem. 2007; 102:96–210.

Mounier N, Arrigo A-P. Actin cytoskeleton and small heat shock proteins: how do they interact? Cell Stress and Chaperones. 2002; 7:167–176. [PubMed: 12380684]

Nomura N, Nomura M, Sugiyama K, Hamada J-I. Phorbol 12-myristate 13-acetate (PMA)-induced migration of glioblastoma cells is mediated via p38MAPK/Hsp27 pathway. Biochem. Pharmacol. 2007; 74:690–701. [PubMed: 17640620]

Påhlman S, Hoehner JC, Nånberg E, Hedborg F, Faerström, Gestblom C, Johansson I, Larrson U, Lavenius E, Örtoft E, Soderhölm H. Differentiation and survival influences of growth factors in human neuroblastoma. Eur. J. Cancer. 1995; 31A:453–458. [PubMed: 7576944]

Rogalla T, Ehrnsperger M, Preville X, Kotlyarov A, Lutsch G, Ducasse C, Paul C, Wieske M, Arrigo A-P, Buchner J, Gaestel M. Regulation of Hsp27 oligomerization, chaperone function, and protective activity against oxidative stress/tumor necrosis factor α by phosphorylation. J. Biol. Chem. 1999; 274:18947–18956. [PubMed: 10383393]

Rosethorne EM, Nahorski SR, Challiss RAJ. Regulation of cyclic AMP response-element binding-protein (CREB) by $G_{q/11}$-protein-coupled receptors in human SH-SY5Y cells. Biochem. Pharmacol. 2008; 75:942–955. [PubMed: 18036509]

Rösner H, Vacun G, Rebhan M. Muscarinic receptor-mediated induction of actin-driven lamellar protrusions in neuroblastoma cell stomata and growth cones. Involvement of protein kinase C. Eur. J. Cell Biol. 1995; 66:324–334. [PubMed: 7656899]

Ross RA, Spengler BA, Biedler JL. Coordinate morphological and biochemical interconversion of human neuroblastoma cells. J. Natl. Cancer Inst. 1983; 71:741–749. [PubMed: 6137586]

Rössler OG, Henss I, Thiel G. Transcriptional response to muscarinic acetylcholine receptor stimulation: regulation of Egr-1 biosynthesis by ERK, Elk-1, MKP-1 and calcineurin in carbachol-stimulated human neuroblastoma cells. Arch. Biochem. Biophys. 2008; 470:93–102. [PubMed: 18061571]

Rouse J, Cohen P, Trigon S, Marnage M, Alonso-Llamazares A, Zamanillo D, Hunt T, Nebreda AR. A novel kinase cascade triggered by stress and heat shock that stimulates MAKAP kinase-2 and phosphorylation of the small heat shock proteins. Cell. 1994; 78:1027–1037. [PubMed: 7923353]

Sharlow ER, Girdhar KV, LaValle CR, Chen J, Leimgruber S, Barrett R, Bravo-Altamirano K, Wipf P, Lazo JS, Wang QJ. Potent and selective disruption of protein kinase D functionality by a benzoxoloazapinolone. J. Biol. Chem. 2008; 283:33516–33526. [PubMed: 18829454]

Sharp PS, Akbar MT, Bouri S, Senda A, Joshi K, Chen HJ, Latchman DS, Wells DJ, deBellroche J. Protective effects of heat shock protein 27 in a model of ALS occur in the early stages of disease progression. Neurobiol. Dis. 2008; 30:42–55. [PubMed: 18255302]

Sheik-hamad D, Gustin MC. MAP kinases and the adaptive response to hyperosmolarity: functional preservation from yeast to mammals. Am J. Phys. Renal. 2004; 287:1102–1111.

Shimura H, Miura-Shimura Y, Kosik KS. Binding of tau to heat shock protein 27 leads to decreased concentration of hyperphosphorylated tau and enhanced cell survival. J. Biol. Chem. 2004; 279:17957–17962. [PubMed: 14963027]

Slack BE. The m3 muscarinic acetylcholine receptor is coupled to mitogen-activated protein kinase via protein kinase C and epidermal growth factor receptor kinase. Biochem. J. 2000; 348:381–387. [PubMed: 10816433]

Slack BE, Blusztajn JK. Differential regulation of mTOR-dependent S6 phosphorylation by muscarinic acetylcholine receptor function. J. Cell Biochem. 2008; 104:1818–1831. [PubMed: 18348264]

Tang X, Batty IH, Downes CP. Muscarinic receptors mediate phospholipase C-dependent activation of protein kinase B via Ca^{2+}, ErbB3, and phosphoinositide 3-kinase in 132N1 astrocytoma cells. J. Biol. Chem. 2002; 277:338–344. [PubMed: 11694521]

Takai S, Matsushima-Nishiwaki R, Tokuda H, Yasuda E, Toyoda H, Kaneoka Y, Yamaguchi A, Kumada T, Kozawa O. Protein kinase C delta regulates the phosphorylation of heat shock protein 27 in human heptacellular carcinoma. Life Sci. 2007; 81:585–591. [PubMed: 17673262]

Viviani B, Galli CL, Marinovich M. Is actin polymerization relevant to neurosecretion? A study on neuroblastoma cells. Biochem. Biophys. Res. Comm. 1996; 223:712–717. [PubMed: 8687462]

Vlahos CJ, Matter WF, Hui KY, Brown RF. A specific inhibitor of phosphatidylinositol 3-kinase, 2-(4-morpholinyl)-8-phenyl-4H-1-benzopyran-4-one (LY 294002). J. Biol. Chem. 1994; 269:5241–5248. [PubMed: 8106507]

Xie H, Hu L, Li G-Y. SH-SY5Y human neuroblastoma cell line: *in vitro* cell model of dopaminergic neurons in Parkinson's disease. Chin. Med. J. 2010; 123:1086–1092. [PubMed: 20497720]

Yuan J, Rozengurt E. PKD, PKD2 and p38 MAPK mediate Hsp27 serine-82 phosphorylation induced by neurotensin in pancreatic cancer PANC-1 cells. J. Cell. Biochem. 2008; 103:648–662. [PubMed: 17570131]

Zheng C, Lin Z, Zhao ZJ, Yang Y, Niu H, Shen X. MAPK-activated protein kianse-2 (MK2)-mediated formation and phosphorylation-regulated dissociation of the signal complex consisting of p38, MK2, Akt and Hsp27. J. Biol. Chem. 2006; 281:32715–33726.

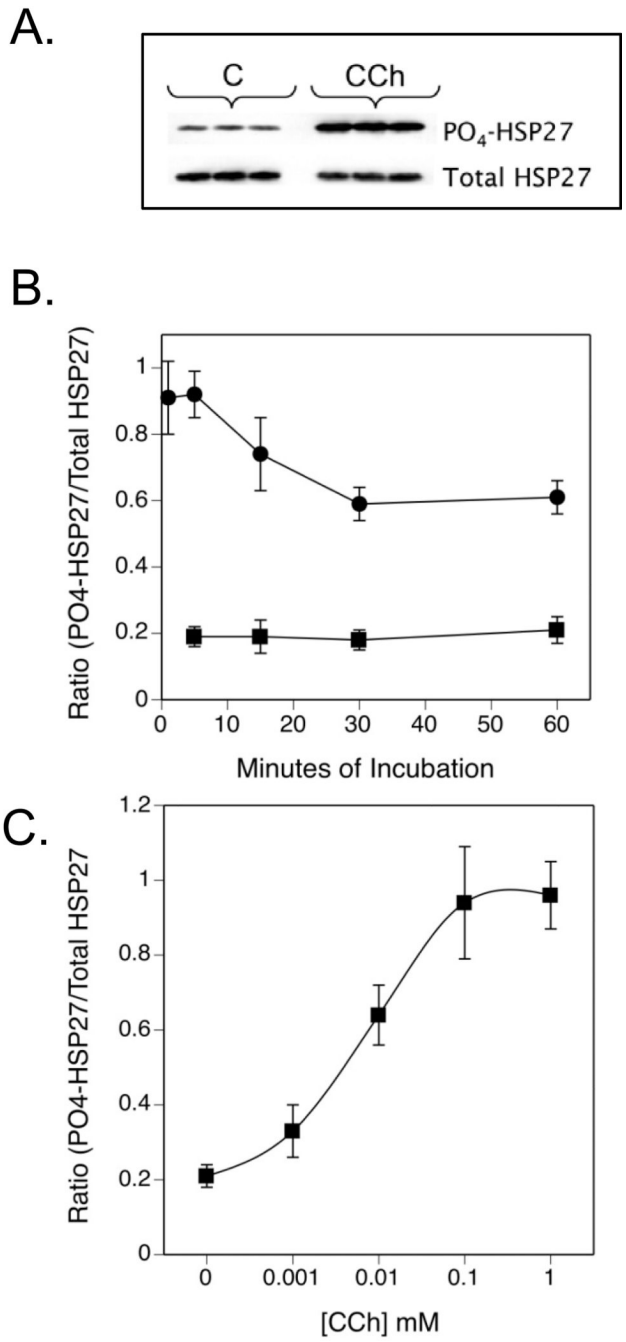

Fig. 1. Carbachol Increases HSP27 Phosphorylation in SH-SY5Y Cells

(**A**.) SH-SY5Y cells were plated at a density of 8×10^5 cells per 60 mm plate and cultured for 2 days when the media was replaced with serum-free DMEM. After a 60 min preincubation, CCh (1 mM) or an equal volume of DMEM (Control, C) were added for 5 min. Portions of cell lysates containing equal amounts of protein were resolved with SDS-PAGE and immunoblotting was performed for phospho-(Ser-82)- or total HSP27. The immunoblotting results shown are from 3 cell plates at each condition. (**B**.) Cells were incubated for the indicated times under control conditions (■ - ■) or with 1 mM CCh (● - ●). (**C**.) Cells were incubated for 5 min with the indicated concentrations of CCh. In panels **B**. and **C**., densitometric results from 3–8 experiments are shown as the mean ± SEM of the

increase in HSP27 phosphorylation normalized to the amount of total HSP27 in each sample.

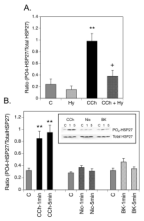

Fig. 2. Carbachol Activates Muscarinic Receptors to Increase HSP27 Phosphorylation in SH-SY5Y Cells

(**A**.) Cells were incubated as described in Fig. 1 except that 1μM hyoscyamine (Hy) was added to some plates 60 min prior to addition of CCh or serum-free DMEM (Control, C) for 5 min. Results shown are the mean ± SEM of the increase in normalized HSP27 phosphorylation at Ser-82 from 3–4 experiments. (**B**.) Cells were preincubated for 1 hr in serum-free DMEM prior to addition of 1mM CCh or nicotine (Nic) or 10^{-7} M bradykinin (BK) for 1 or 5 min. The insert shows a single immunoblot of phospho-(Ser-82)- and total HSP27. Results from 3–4 experiments were combined to obtain the mean ± SEM of the normalized HSP27 phosphorylation. ** $p < 0.01$ as compared to the control value.

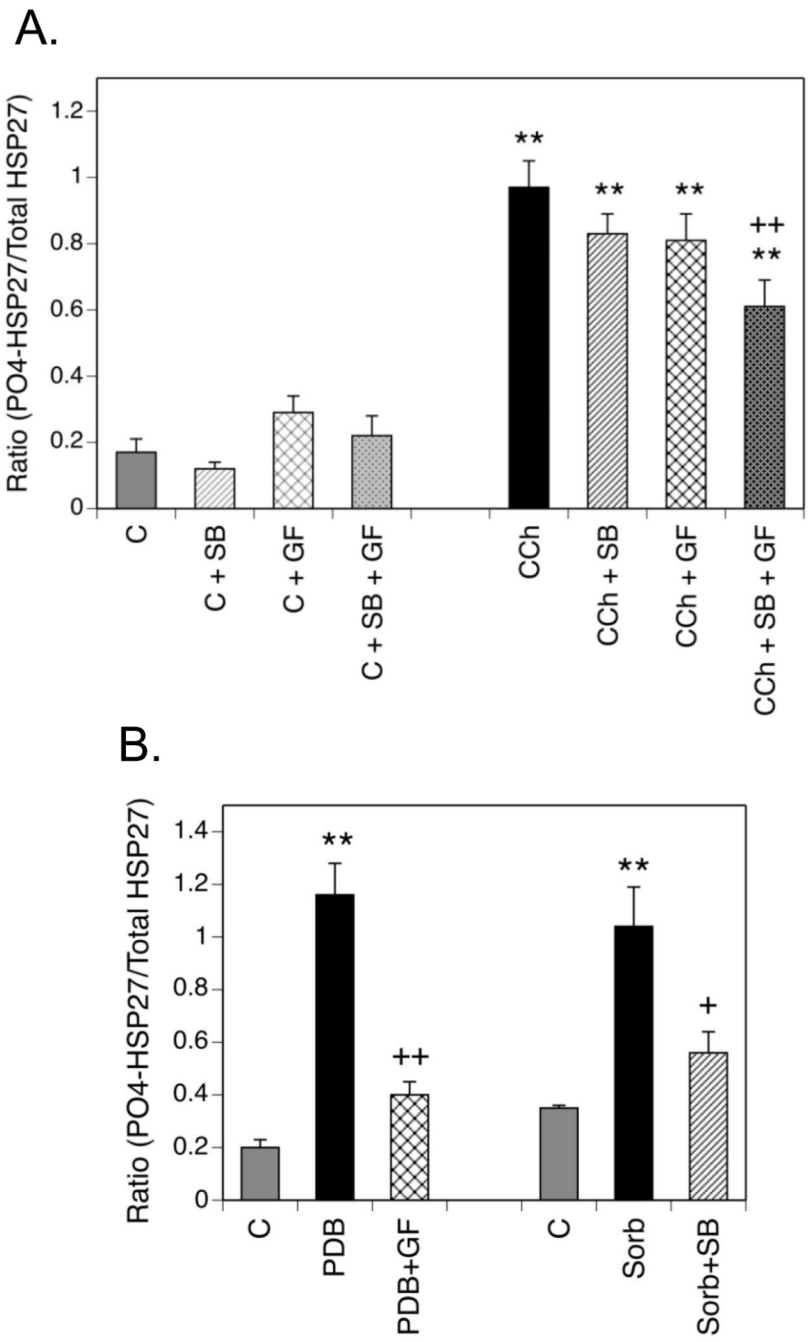

Fig. 3. Phosphorylation of HSP27 is Sensitive to Multiple Stimuli in a Protein Kinase-Specific Manner

(**A**.) SH-SY5Y cells were preincubated with inhibitors of p38 MAPK, SB 203580 (SB, 10 μM) and/or PKC, GF 109203X (GF, 5 μM) or an equal volume of the vehicle, DMSO. Following addition of 1 mM CCh or an equal volume of DMEM (Control, C) for 5 min, cells lysates were prepared. Samples containing equal amounts of protein were resolved with SDS-PAGE prior to immunoblotting for phospho-(Ser-82)- or total HSP27. Results are expressed as the mean ± SEM of normalized HSP27 phosphorylation from 4–8 experiments. (**B**.) Cells were incubated in serum-free DMEM for 60 min with addition of 1 μM PDB during the last 15 min prior to preparation of cell lysates. In different samples, the medium

was changed at 30 min to include 0.3 M sorbitol (Sorb) to induce hyperosmotic conditions. At this time, the serum-free DMEM on control (C) plates was also replaced. Where indicated, protein kinase inhibitors (GF or SB) were present throughout the incubation. Equal volumes of the DMSO vehicle for PDB and the protein kinase inhibitors were added to control (C) plates. Immunoblotting results from 5 or 6 experiments of this type were analyzed with densitometry to obtain the mean ± SEM of normalized HSP27 phosphorylation. ** $p < 0.01$ as compared to the control value; $^{+}$ $p < 0.05$ as compared to the CCh value; $^{++}$ $p < 0.01$ as compared to the CCh value.

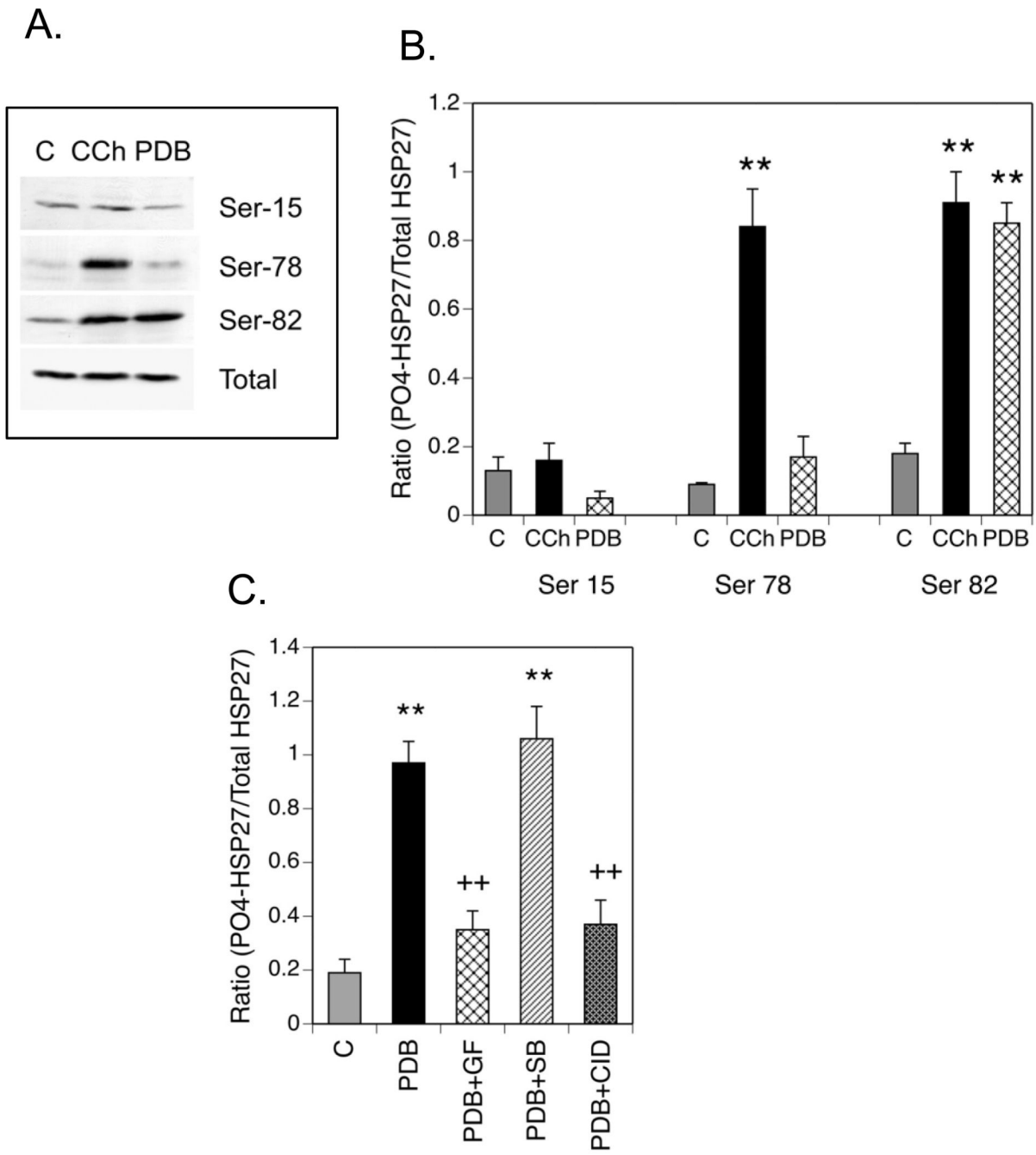

Fig. 4. Comparison of HSP27 Phosphorylation in Response to Carbachol or Phorbol Ester

(**A**.) SH-SY5Y cells were incubated under control (C) conditions, with 1 mM CCh or with 1 μM PDB as described in Fig. 3. Portions of the cell lysates were resolved with SDS-PAGE and immunoblotting was performed for HSP27 with phospho-specific antibodies directed against Ser-15, Ser-78 and Ser-82 or an antibody to total HSP27. (**B**.) Immunoblotting results from 4 experiments of this type were analyzed with densitometry to obtain the mean ± SEM of normalized HSP27 phosphorylation. (**B**.) SH-SY5Y cells were cultured and preincubated with inhibitors of PKC [GF 109203X (GF, 5 μM)], p38 MAPK [SB 203580 (SB, 10 μM)] or PKD [CID 755673 (CID, 25 μM)] or an equal volume of the vehicle, DMSO. Following incubation for 45 min, 1 μM PDB or an equal volume of DMSO

(Control, C) were added for 15 min and cell lysates were prepared. Samples containing equal amounts of protein were resolved with SDS-PAGE prior to immunoblotting for phospho-(Ser-82)- or total HSP27. Results are expressed as the mean ± SEM of normalized HSP27 phosphorylation from 4–6 experiments. ** $p< 0.01$ as compared to the control value; $^{++}$ $p< 0.01$ as compared to the PDB value.

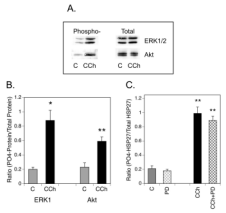

Fig. 5. Muscarinic Receptor Activation Increases ERK1/2 and Akt Phosphorylation in SH-SY5Y Cells

SH-SY5Y cells were cultured and incubated as described in Fig. 1. ± 1mM CCh. (**A**.) Following lysis, cell samples containing equal amounts of protein were resolved with SDS-PAGE and immunoblotting was performed for total and phosphorylated forms of ERK1/2 (Thr-202/Tyr-204) or Akt (Ser-473). Representative sets of immunoblots for each protein are shown. (**B**.) Immunoblotting results from 3 (ERK1/2) or 5 (Akt) experiments of this type were analyzed with densitometry to obtain the mean ± SEM of normalized phosphorylation. Since similar results were obtained for ERK1 and ERK2, only the former protein was used for densitometric analysis. (**C**.) Cells were preincubated with a MKK inhibitor, PD 98059 (PD, 10 μM) for 60 min or an equal volume of serum-free DMEM (Control, C) prior to addition of 1mM CCh for 5 min. HSP27 phosphorylation at Ser-82 and total HSP27 were determined with immunoblotting. Densitometric results are expressed as the mean ± SEM of the increase in normalized HSP27 phosphorylation from 4–8 experiments of this type. * $p < 0.05$ as compared to the control value; ** $p < 0.01$ as compared to the control value.

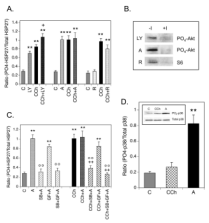

Fig. 6. Phosphorylation of HSP27 is Modulated by Inhibition of PI3-K or Akt

(**A**.) Cells were incubated ± LY 294002 (LY, 50 μM), Akti-1/2 (A, 10 μM) or rapamycin (R, 0.1 μM) for 60 min prior to addition of CCh for 5 min. Control incubations (C) contained equal volumes of the vehicles for CCh and/or the inhibitors. (**B**.) To confirm the activities of LY, A and R, cells were incubated ± these protein kinase inhibitors for 60 min prior to addition of 1 mM CCh or a corresponding volume of serum-free DMEM for 5 min. Lysates were prepared, resolved with SDS-PAGE and immunoblotting was performed for phospho-(Ser-473)-Akt or phospho-(Ser-235/236)-S6 ribosomal protein. (**C**.) Cells were preincubated with Akti-1/2 alone or in combination with SB 203580 (SB, 10 μM) and/or GF 109203X (GF, 5 μM) for 60 min prior to addition of 1 mM CCh or an equal volume of serum-free DMEM for 5 min. Immunoblotting was performed on cell lysates for phospho-(Ser-82)- and total HSP27. (**D**.) SH-SY5Y cells were incubated under control (C) conditions or with 1 mM CCh for 5 min following a 60 min preincubation or with 10 μM Akti-1/2 (A) for 60 min. Cell lysates were prepared and immunoblotting was performed with a phospho-specific antibody directed against Thr-180/Tyr-182 in the activation domain of p38 MAPK or with an antibody that recognizes p38 MAPK independent of its phosphorylation state. The insert is a representative blot showing amounts of phospho- and total p38 MAPK in one experiment. Results shown are the mean ± SEM of normalized phosphorylation from 3–12 experiments. ** $p < 0.01$ as compared to the control value; $^{+}p < 0.05$ as compared to the CCh value; $^{++}p < 0.01$ as compared to the CCh value; $^{oo}p < 0.01$ as compared to the Akti-1/2 value.

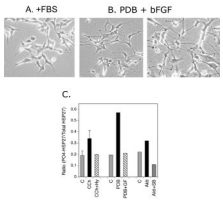

Fig. 7. HSP27 Phosphorylation in Differentiated SH-SY5Y Cells

(**A**.) SH-SY5Y cells were grown under standard conditions (DMEM-10% FBS-penicilin/streptomycin for 2 days. (**B**.) Twenty-four hr after plating of SH-SY5Y cells, the medium was changed to serum-free DMEM containing 16 nM PDB and 3 nM bFGF. These conditions were maintained for 5 days. Cells grown under both conditions were imaged with phase contrast microscopy. (**C**.) Cells were differentiated, preincubated with hyoscyamine (Hy, 1 μM), GF 109203X (GF, 5 μM), Akti-1/2 (A, 10 μM) ± SB 203580 (SB, 10 μM) or DMSO vehicle. CCh (1 mM) or PDB (1 μM) were added for 5 min or the last 15 min of the preincubation, respectively. Lysates were prepared, equal volumes of protein were resolved with SDS-PAGE amd immunoblotting was performed for phospho-(Ser-82)-HSP27 or total HSP27. Normalized results were averaged (± SEM) from 3 experiments with CCh and duplicate experiments under all other conditions.

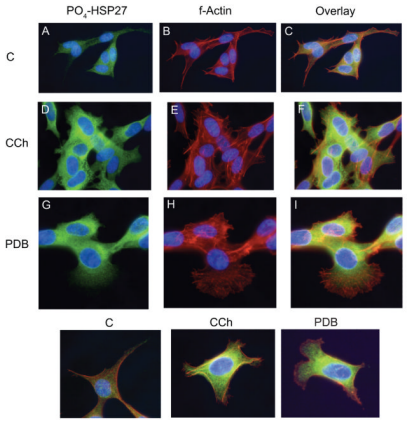

Fig. 8. Muscarinic Receptor Activation and Phorbol Ester Increase Phospho-HSP27 Immunofluorescence and Alter the Actin Cytoskeleton in SH-SY5Y Cells

SH-SY5Y cells were cultured for 2 days post-plating on glass coverslips. The medium was changed to serum-free DMEM 60 min prior to addition of CCh (**D., E., F**.) to a final concentration of 1 mM for 5 min or 1 μM PDB (**G., H., I**.) for the last 15 min of the preincubation. Control cells (**A., B., C**.) were incubated for the same times with an equal volume of the corresponding vehicle (serum-free DMEM or DMSO). Cells were fixed, permeabilized and immunolabeled for phospho-(Ser-82)-HSP27 [Green: (**A. D., G)**] and stained for f-actin with rhodamine phalloidin [Red: **B., E., H**.)]. Cell nuclei were counterstained with DAPI (Blue). Images were obtained at the same resolution and exposure time and are representative of triplicate experiments with each concentration and time of incubation with CCh or PDB. **Bottom Panel:** SH-SY5Y cells, grown on glass coverslips, were incubated with CCh or PDB as described. The double labeled images shown were selected to emphasize the distribution of phospho-(Ser-82)-HSP27 (Green) and f-actin (Red) in individual cells.

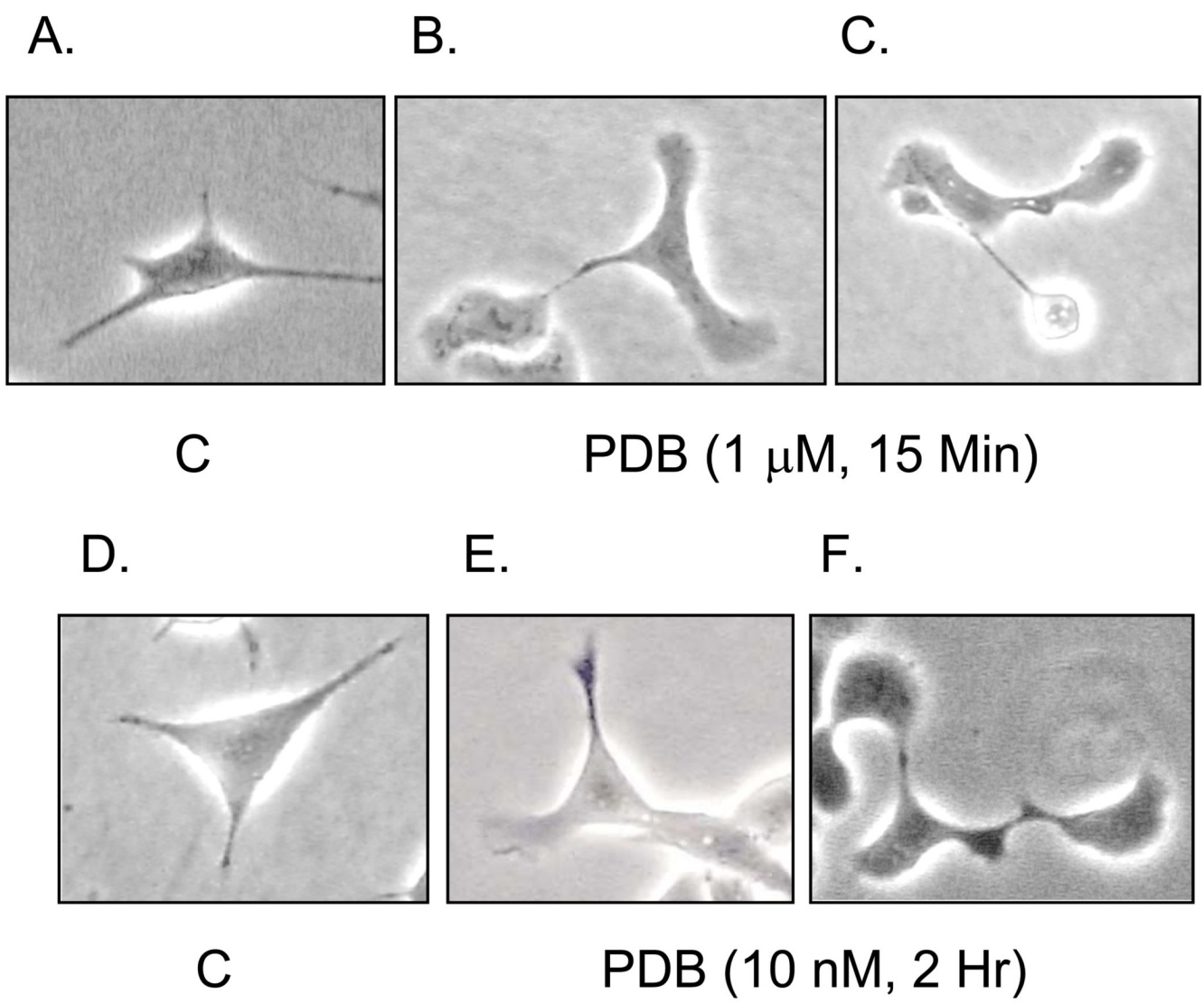

Fig. 9. Activation of PKC Changes SH-SY5Y Cell Morphology to a Lamellipodial Phenotype

SH-SY5Y cells were grown on 60 mm polystyrene plates for two days. The medium was replaced with serum-free DMEM and cells were preincubated for 60 min prior to addition of PDB under two conditions: at a concentration of 1 μM for 15 min (**B., C)** or at 10 nM for 2 hr (**E., F)**. Control cells were incubated for the same times with an equal volume of the vehicle, DMSO (**A., D**.). Cell images were then obtained with phase contrast microscopy. The images shown were selected as examples of the morphology typical of control cells or those treated with each concentration of PDB from triplicate experiments.

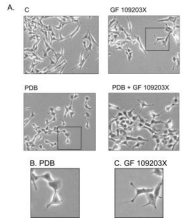

Fig. 10. The Effect of PDB on Cell Morphology is Long-lasting and Reversed by Inhibition of PKC

(**A**.) Two days post-plating, SH-SY5Y cells were preincubated for 60 min ± 5 μM GF 109203X prior to addition of 10 nM PDB for 2 hr or with an equal volume of the vehicle, DMSO (Control, C) for 2 hr. Cells were imaged with phase contrast microscopy. The single cells shown in the boxed areas in (**A**.) were enlarged to show typical examples of the morphology induced by PDB (**B**.) or GF 109203X (**C**.) in duplicate experiments.

TABLE I

Selectivity of protein kinase inhibitors[a]

Inhibitor	Protein Kinase	Concentration	References
SB 203580	α- and β-p38 MAPK	10 μM	Cuenda et al., 1995
GF 109203X	PKC	5 μM	Heikkilä et al. 1993
PD 98059	MKK	10 μM	Kim et al., 1997
LY 294002	PI3-K	50 μM	Vlahos et al., 1994
Akti-1/2	Akt1 and Akt2	10 μM	Barnett et al., 2005
Rapamycin	mTORC1	0.1 μM	Slack and Blusztjn, 2008
CID 755673	PKD	25 μM	Sharlow et al., 2008

[a]The concentrations of protein kinase inhibitors were selected with reference to tabulated data of their target selectivities as determined by Davies et al., 2000 and Bain et al., 2007. More specific information regarding concentrations that achieve effective inhibition of each targeted protein kinase in cultured cells was obtained from the references shown in the Table. The full chemical name of each protein kinase inhibitor is provided in the list of abbreviations.

TABLE II

Effect of protein kinase inhibitors on phorbol ester-induced SH-SY5Y cell morphology

Condition	% Cells with Flared Lamellipodia
Control	1.5 ± 0.8
GF 109203X	0.5 ± 0.2
PDB	43.0 ± 1.5
PDB + GF 109203X	1.5 ± 0.8
Control	1.0 ± 0.9
CID 755673	0 ± 0
PDB	46 ± 2.8
PDB + CID 755673	47.0 ± 3.0

SH-SY5Y cells were cultured at a density of 4×10^5/60 mm plate. Two days after plating, the medium was changed to serum-free DMEM with addition of protein kinase inhibitors for 1 hr at concentrations shown in Table 1. Control plates contained an equal volume of DMSO. Phorbol ester (PDB) was then added for 2 hr at a concentration of 10 nM. Cells were imaged with phase contrast microscopy. For each condition, 50 cells per field were counted for the presence of flared lamellipodia (as shown in Figs. 9 and 10). The results are the average ± SEM from a total of 4 fields from duplicate experiments with each protein kinase inhibitor.